NOAO Director's Corner

David Silva

The level of intellectual energy and excitement at NOAO has increased markedly in the last few months. Everywhere you turn in Arizona and Chile, new projects and ideas are blossoming, creating new research opportunities and capabilities for our user community now and in the near future. Engaging with these new projects and the associated collaborations, hosting national centers, and sponsoring federal agencies has brought new thinking and ideas to NOAO, challenging us to raise our game. March 2015 is a particularly busy period. What's all the excitement about?

Dark Energy Camera (DECam) at the CTIO Blanco 4-m telescope continues to be a huge success. The second year of Dark Energy Survey (DES) observations has been completed with mean image quality and higher observing efficiency than the first year; raw and processed images from the first year of DES observations are now available through the NOAO Science Archive (see two related articles in this issue). DES object catalogs will become publicly available in mid 2017. Meanwhile, the community–at-large is using DECam for a wide range of research projects from characterizing the low end of the Near-Earth Object size distribution to determining mass distribution maps for high-mass galaxy clusters at intermediate redshift. Particularly noteworthy, the DECam Legacy Survey (DECaLS) is creating a major public data set by imaging the entire Sloan Digital Sky Survey (SDSS) footprint south of the 30-degree declination in *grz* at least two magnitudes deeper than SDSS. The first release of DECaLS processing images and object catalogs is planned for March 2015. None of these projects would have been possible just a few years ago (before DECam). To help maximize the impact of this magnificent instrument, NOAO is holding a community workshop, "DECam Community Science Workshop," on March 11–13, to showcase early science results and to enable communication and cross-fertilization within the DECam user community.

Just providing processed images and catalogs, however, is no longer enough. Our user community expects to have better tools for data exploration, visualization, and manipulation. Therefore, a new project known as the NOAO Data Lab has been launched. The Data Lab project strives to allow users of large NOAO-hosted data sets (yes, NOAO's archive has reached the petascale) to explore imaging and spectral data sets with their associated catalogs, experiment with and conduct complex workflows applied to those data sets, and allow collaborators to see and share all steps of that analysis. The goal is not to reinvent existing tools and systems but to adapt and deploy them for use by the NOAO community in collaboration with other groups. A Conceptual Design Review is scheduled for mid-March. If all goes well, the initial public release will occur by mid 2017 to correspond to the first public release of the DES catalogs. To further educate ourselves and our community about the challenges of conducting research with large astronomical data sets, NOAO is holding a workshop, "Tools for Astronomical Big Data," on March 9–11, to survey the present state of the art in addressing the challenges of conducting research with large astronomical data sets.

Also in March, Cornell University will deliver TripleSpec4 to the CTIO Blanco 4-m telescope. A cross-dispersed near-IR spectrometer, TripleSpec4 will cover 0.8–2.45 μm simultaneously at R ~ 3200. If all goes well, this instrument will be available to the community for the 2016A observing semester. The arrival of TripleSpec4 closely follows the release of the new, multi-mode optical spectrometer COSMOS (CTIO Ohio State Multi-Object Spectrometer) at the Blanco. The Blanco instrument suite (DECam, COSMOS, TripleSpec4) has been completely renewed to a world-class state and lays the foundation for Blanco-based research in the era of the Large Synoptic Survey Telescope (LSST).

Another exciting development is the advent of the NASA-NSF Exoplanet Observational Research program (NN-EXPLORE). At the heart of this program will be the deployment of an extreme precision Doppler spectrometer (EPDS) at the WIYN 3.5-m telescope on Kitt Peak. NASA has recently issued a request for EPDS proposals. A pre-proposal meeting will be held in March. NOAO will be deeply involved in integrating this instrument into the WIYN facility and operating it.

Meanwhile, the Dark Energy Spectroscopic Instrument (DESI) project continues to make good progress, including a successful Critical Decision 1 (CD-1) review by the Department of Energy in late 2014. Currently, all major optical elements (six of them) of the prime focus corrector are in fabrication. Components of the prototype spectrograph (a three-arm design) will be delivered during 2015, and preparations for a prototype system to test the fiber positioners and acquisition camera (proto-DESI) are being made. Analogous to DECam, NOAO is responsible for preparing the Mayall facility on Kitt Peak for DESI installation, after which NOAO will be deeply involved in the installation, commissioning, and operation of DESI.

The construction start for LSST also has also injected new energy into NOAO. The LSST Project Office team is moving into office spaces renovated for them at NOAO's sites in Arizona and Chile, strengthening the bridge between the NOAO and LSST teams. Furthermore, site preparation work is moving at a high tempo on Cerro Pachón in Chile. Because the Data Lab is in many ways a pathfinder project for working with LSST-scale data sets, there is growing LSST/NOAO synergy in that arena, as well.

Looking further into the future at the Thirty Meter Telescope (TMT), the NOAO TMT Liaison Office is working with community scientists to provide input into a federal participation plan being developed by the TMT Project team within the framework of a cooperative agreement between NSF and TMT. That plan will include the scientific justification for TMT from the perspective of the US community, the TMT technical capability and operational requirements that flow from that justification, and how federal participation in TMT can address broader impacts in the areas of workforce development, education, and public outreach.

New collaborations, new major instruments and data sets, new data services under development, continued involvement in LSST, renewed connections to TMT are all signs of a healthy, vigorous NOAO program—a program that will enable excellent community-based research into the mid 2020s and beyond.

Massive Galaxy Clusters as Test Bed for the Dark Energy Survey

Peter Melchior (Ohio State University/CCAPP) for the DES collaboration

Peter Melchior (OSU/CCAPP) and a large team of Dark Energy Survey (DES) collaborators used the Dark Energy Camera (DECam) on the CTIO 4-m telescope to study four massive galaxy clusters. The targeted clusters were well known so that the findings from DECam could be cross-checked with existing results. The team chose to validate the demanding technique of weak gravitational lensing to infer integrated cluster masses and two-dimensional mass distributions. This presented a formidable challenge because weak lensing has stringent requirements on image quality as well as astrometric accuracy and photometric uniformity. Because weak lensing is encoded in imperceptibly small changes in galaxy sizes and ellipticities, the first test for any successful analysis is how well the telescope's point spread function (PSF) can be modeled. While stellar ellipticities could be modeled accurately, getting the stellar sizes correct proved to be a harder problem. The bulk of all stars appeared to be ~1% smaller than the model that was built from them. This mismatch is due to the thick, fully depleted CCDs used in DECam, which have a mild flux-dependent registration of charges, the so-called "brighter-fatter" effect. The few very bright stars, which dominate the PSF model, create so many charges in the central pixels that newly incoming charges get slightly repelled by the charges already present, causing the PSF to be broader than that measured from faint stars. Thus, to build precise PSFs, the brightest stars had to be rejected.

Combining weak-lensing measurements with photometric redshift (photo-z) values for the background galaxies, one can infer the mass of the cluster that acts as lens. Figure 1 shows the mean tangential ellipticity, the primary weak-lensing signal, as a function of separation from the Brightest Cluster Galaxy (BCG) of the cluster RXC J2248.7-4431 (z = 0.348). Also shown are 100 Markov chain Monte Carlo (MCMC) samples of Navarro-Frenk-White (NFW) profile fits to the data, a standard choice to describe the radial profile of dark matter haloes. The parameters of this model are the mass M_{200c} enclosed in a given aperture (the sphere that contains 200× the critical density of the universe at the cluster redshift) and the concentration c_{200c} that describes the slope of the profile within the same aperture. The resulting fit yields a cluster mass in good agreement with previously published results. Moreover, the team could show that the cluster mass estimates remained unchanged when the weak-lensing measurements were done in any of the *riz* filters, demonstrating that the team accounted for all relevant instrumental effects.

Figure 1 also demonstrates that the NFW profile is often not a good fit to individual clusters, whose mass distributions may deviate from any spherical model. Indeed, the contours in the left panel of Figure 2 show the 2-D mass distribution as inferred from weak lensing (a so-called aperture-mass M_{ap} map in units of its dispersion) in an area of 30′ × 30′, revealing a strongly elongated cluster. Also shown (as black dots) are red-sequence galaxies at the redshift of the cluster, identified by the REDMAPPER code (Rykoff et al. 2014). Their redshift estimates from five-band *grizY* imaging of DES are found to exhibit a scatter of only 0.015, significantly more precise than the typical DES photo-z scatter of ~0.1. As another confirmation of a successful lensing analysis, the mass distribution of the cluster is tightly traced by its red-sequence galaxy distribution. With the accuracy of the red-sequence redshifts, the DES data allowed the team to connect the central cluster region to its larger-scale environment, literally by following a string of galaxies. The right panel in Figure 2 shows the same red-sequence galaxies as the central panel, in a narrow redshift slice, for an area of 90′ × 90′. It became evident that this massive cluster is embedded in a filamentary structure that spans about 12 Mpc toward another, less massive cluster (red diamond). The Bullet Cluster, the other very massive and actively merging cluster in the sample, showed a similarly rich environment. That filaments connect clusters, particularly the very massive ones, is not news: it had been predicted from simulations and observed spectroscopically. But, being able to map out the cluster environment without spectroscopy bears truly exciting prospects for large-scale structure studies in the 5000 square degrees of DES.

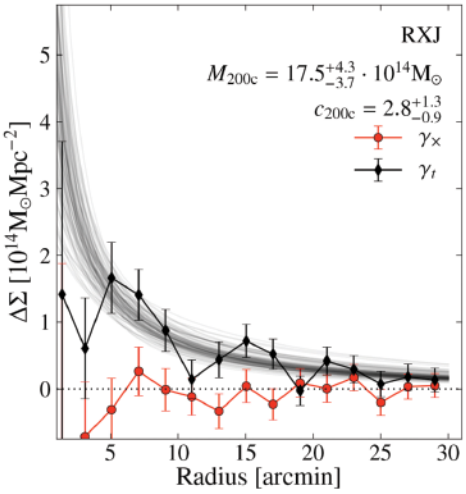

Figure 1: Mean ellipticity γ_t (black) in the tangential direction (with respect to the cluster center) in terms of excess surface mass density $\Delta\Sigma$ as a function of the distance from the brightest cluster galaxy (BCG) of the cluster RXC J2248.7-4431. Also shown are the B-mode $\gamma_\times$ (red) and 100 MCMC samples of NFW fits to the data. The B-mode $\gamma_\times$ cannot be generated by gravitational lensing and thus serves as a null test. The mean and 68% confidence intervals for the integrated mass M_{200c} and halo concentration c_{200c} for the NFW model (listed in the upper right corner) are in good agreement with previously published results for this cluster.

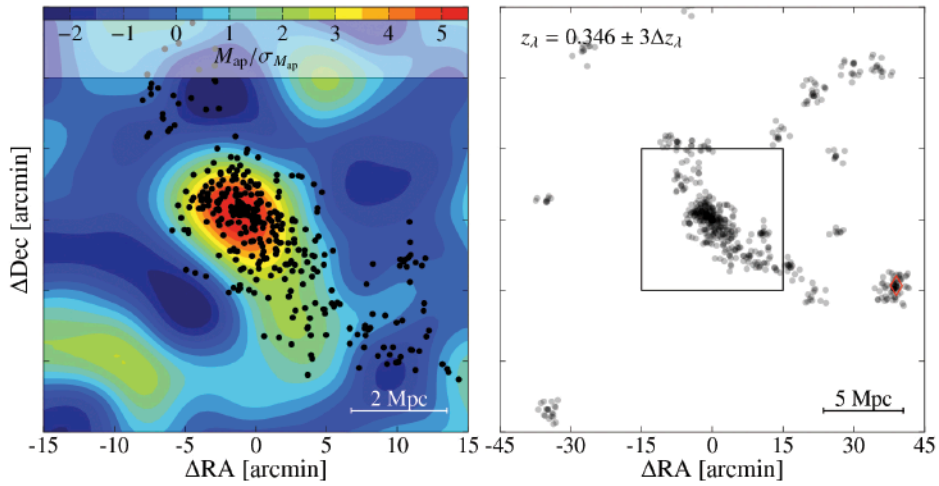

Figure 2: (Left:) Weak-lensing mass map of the inner 30′ × 30′ (contours), overlaid with red-sequence galaxies (black dots) in REDMAPPER-detected groups of at least five members in a narrow redshift slice around the cluster RXC J2248.7-4431. (Right:) The same REDMAPPER galaxies but for the entire useable field of view of 90′ × 90′. The panels are centered on the BCG; the size of the left panel is indicated by a black box on the right.

Connecting the Dots with KOSMOS

Alec S. Hirschauer (Indiana University)

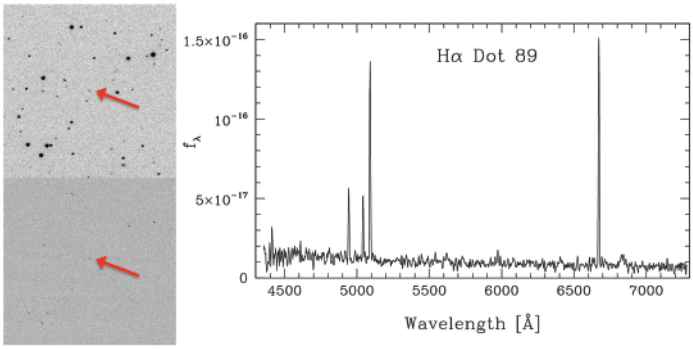

Figure 1: Example images of an Hα-selected Hα Dot: R-band continuum and continuum-subtracted Hα image taken with the WIYN 0.9-m telescope, with a quick-look spectrum taken using the 9.2-m Hobby Eberly Telescope. Hα Dots are serendipitously detected in continuum-subtracted narrowband Hα images taken for the ALFALFA Hα survey. Emission for these objects corresponds to Hα in a similar velocity range to the original target galaxy, but these objects are independent systems.

Alec S. Hirschauer and John J. Salzer (Indiana University) used the new KPNO Ohio State Multi-Object Spectrograph (KOSMOS) on the Mayall 4-m telescope to observe a set of fifteen Hα "Dots." These objects are serendipitously detected in continuum-subtracted narrowband Hα images taken for the ALFALFA Hα survey (Van Sistine et al. 2015; based in part on the NOAO Survey Program "Making Hay with ALFALFA").

Point-like emission falling within the survey's narrowband filter that is not obviously associated with the target ALFALFA galaxy is designated as an Hα Dot, typically falling into one of three categories (Figure 1): (1) Hα-detected low-redshift dwarf star-forming galaxies, (2) intermediate-redshift [O III]-selected star-forming galaxies and Seyfert 2s, or (3) high-redshift quasi-stellar objects (QSOs). The subset of Hα-selected Hα Dots includes some of the lowest-luminosity star-forming galaxies in the local Universe; all fifteen Hα Dots observed for this study belong to this group. Observational work on such objects offers a unique opportunity to study the physics of star formation at extremely low luminosities.

To study the chemical enrichment of low-luminosity star-forming systems, fifteen Hα Dots were observed using KOSMOS in long-slit mode. These targets were selected because they possessed strong enough [O III] λ5007 Å in quick-look spectra that the temperature-sensitive auroral [O III] λ4363 Å line should be detectable. This line is necessary for electron temperature (T_e) direct-method determination of the abundance of the nebular gas. These galaxies exhibit a range of *R*-band apparent magnitudes between 17.3 and 21.0, and are at distances between 65 and 100 Mpc. Observations were made using both the Blue grism (2500–6200 Å) and Red grism (5000–9000 Å). The resulting nebular spectra are of exceptional quality (Figure 2).

Figure 3 shows the placement of the emission line flux ratio data onto a standard line-diagnostic diagram (Baldwin, Phillips, & Terlevich 1981). The solid line is a star-formation sequence for high-excitation objects from Dopita & Evans (1986), while the dashed line represents an empirically derived demarcation between star-forming galaxies and active galactic nuclei (AGN) from Kauffmann et al. (2003). The location of

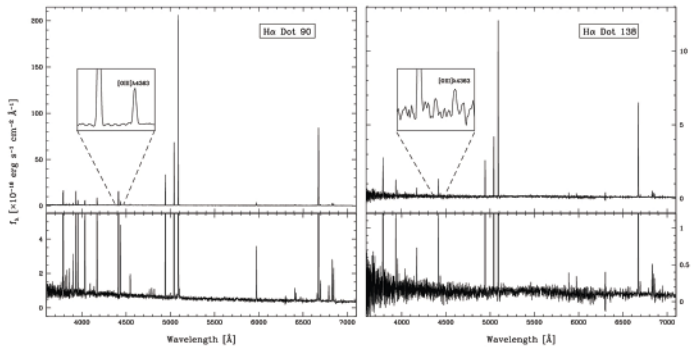

Figure 2: Optical spectra of Hα Dots 90 and 138 observed using KOSMOS. Inset boxes show [O III] λ4363 Å for determinations of T_e abundances. While Hα Dot 90 is relatively bright, Hα Dot 138 is among the lowest-luminosity targets in this sample.

the Hα Dots on this plot confirms the nature of these targets as fairly high-excitation, low-abundance star-forming systems. Those points with a black ring represent targets for which [O III] λ4363 Å was measured, enabling a determination of the electron temperature. Oxygen abundances have been calculated for all eleven Hα Dots with detected [O III] λ4363 Å, falling into the range of $7.74 < 12+\log(O/H) < 8.17$.

With robust oxygen abundance measurements made for 11 systems, this sample of Hα Dots may then be used to study dwarf star-forming galaxy metallicity relations on the low-luminosity end. The relationship between a galaxy's chemical enrichment and its stellar content has been known for several decades (e.g., Lequeux et al. 1979); however,

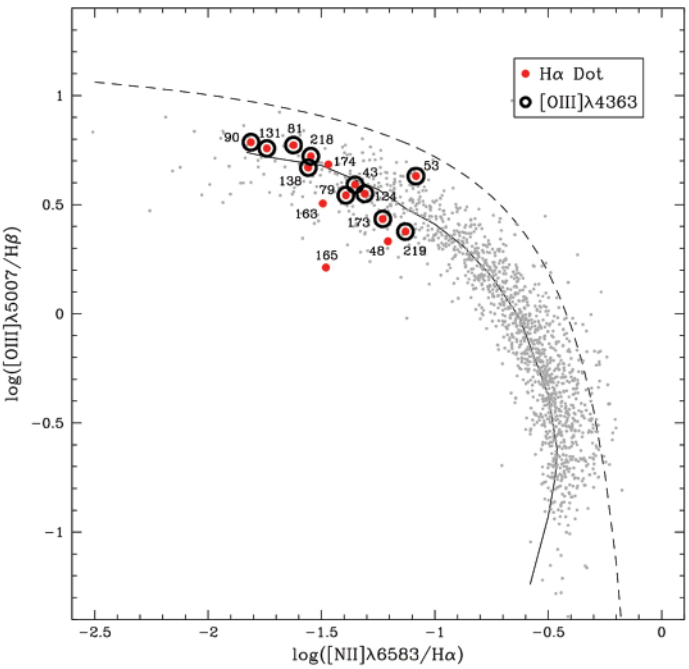

Figure 3: Diagnostic diagram showing location of 15 Hα Dots observed using KOSMOS (red) with those for which we measured [O III] λ4363 Å (black rings). Gray points represent star-forming galaxies from the KPNO International Spectroscopic Survey (KISS) (Salzer et al. 2000).

continued

Connecting the Dots with KOSMOS continued

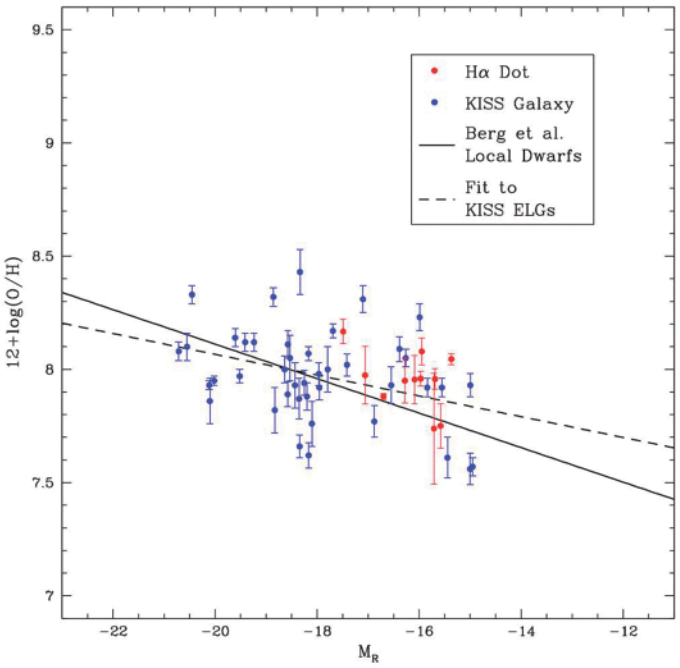

observational data points with robust metallicity calculations on the faint end are comparatively scarce. The luminosity-metallicity (L-Z) diagram of Figure 4 illustrates the location of the Hα Dots from this study (red) against star-forming galaxies with T_e abundances from the KISS survey (blue), which are detected using similar methods. On this plot, the solid line represents an L-Z fit to local dwarf galaxies converted to *R*-band luminosities from Berg et al. (2012), while the dashed line represents a direct fit to the KISS galaxies. The new KOSMOS spectra have added several data points to the faint end of the L-Z relation. These preliminary results are just a small taste of the future promise of this program. A sample of Hα Dots for the spring includes many more compact star-forming objects at even lower luminosities than were observed last fall.

Figure 4: *R*-band luminosity-metallicity (L-Z) relation diagram with star-forming galaxies from KISS (blue) and Hα Dots (red). The solid line represents an L-Z fit to local dwarf galaxies converted to *R*-band luminosities from Berg et al. (2012), while the dashed line represents a direct fit to the KISS galaxies.

Water at the Center of a Transitional Protoplanetary Disk – Where It Shouldn't Be!

Colette Salyk (NOAO)

The Texas Echelon Cross Echelle Spectrograph (TEXES) visitor instrument (PI: J. Lacy) on Gemini North was used by a US-based observing team, led by Colette Salyk (NOAO), to detect water vapor in the inner region of a type of protoplanetary disk known as a "transition disk." Transition disks have inner regions depleted of small dust grains, as detected with spectral energy distributions and millimeter-wave interferometric images. The depleted regions in many transition disks are due likely to dynamical interactions with one or more planets, which tidally clear the disk material in their vicinity. However, the inner regions of transition disks display a diversity of both physical and chemical properties, and it is not yet understood exactly how the growing planets interact with and affect their environment.

An interesting potential tracer of this inner disk region is water vapor. This molecule is easily dissociated in the presence of ultraviolet (UV) radiation and so depends on dust shielding and high densities (which allow for fast chemical formation) to survive. While a high percentage of protoplanetary disks harbor water vapor in their inner disk, nearly all transition disks have dry inner regions, in spite of retaining some CO gas. Therefore, for these transition disks, the formation of planets and the subsequent removal of disk material has created an environment hostile for the survival of water vapor, and radically changed the local chemistry.

continued

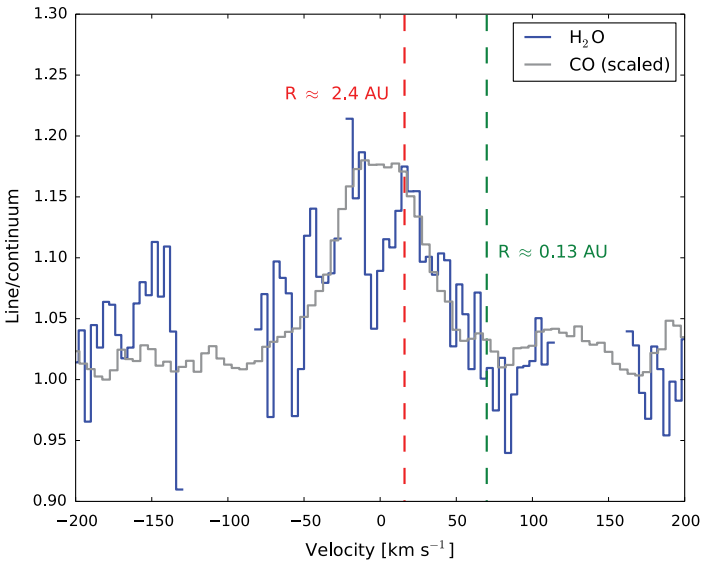

Binned composite emission lines for water vapor (with TEXES; blue) and CO (with NIRSPEC; gray) confirm that the inner, depleted region of the DoAr 44 disk actually contains both CO and water vapor. TEXES is the only instrument able to provide these water vapor observations, thanks to its extremely high spectral resolution and mid-infrared capabilities.

Water at the Center of a Transitional Protoplanetary Disk continued

The target of this work is one exception to this rule. DoAr 44—a young K-type star in the approximately 3-Myr-old Ophiuchus star forming region—is surrounded by a transition disk that shows, using the Spitzer-Infrared Spectrogram (Spitzer-IRS), a spectrum rich with warm water vapor. However, with the spectrally and spatially unresolved Spitzer-IRS spectrum alone, we cannot definitively say whether the water vapor arises in the inner, planet-forming region of the disk. TEXES is unique in providing high spectral resolution (up to R ~ 100,000) at mid-infrared wavelengths, where water vapor emits strongly. With TEXES, we detected spectrally-resolved emission lines from DoAr 44 and used the kinematic information to determine that the water vapor originates in the inner disk—likely interior to where any giant planets have formed.

Future work will determine the gas/dust and water/CO ratios in this region and provide an understanding of why this transition disk has remained water vapor rich, while others are depleted of their water vapor. In particular, we suspect that the planets in this disk have allowed a gas and dust-rich ring of material to remain in the inner disk, perhaps due to the particular configuration or masses of the young planets. In addition, these results could have interesting implications for the formation of terrestrial planets, as they suggest that the chemical environment in which the terrestrial planets form depends sensitively on the influence of faster-forming giant planets.

A Forming Planet and Its Circumplanetary Disk

Joan Najita (NOAO)

Planets are found to occur commonly around low-mass stars, but little is known observationally about how planets form. Only a few candidate-forming planets have been identified to date. In a recent paper (Brittain et al. 2014, ApJ, 791, 136), we reported possible evidence for a forming planet, surrounded by a circumplanetary disk, that orbits the young Herbig Be star HD100546. The results provide, perhaps, the first evidence that planets are surrounded by a circumplanetary disk at birth.

By analyzing multiple epochs of high resolution 5 μm CO spectroscopy of HD100546, obtained over 10 years, we identified the spectroastrometric signature of a component of hot CO emission that orbits the star at a radius of ~13 AU and has the expected emitting area of a circumplanetary disk. HD100546 is a B9e star, 3–10 Myr old, at a distance of ~97 pc.

Circumplanetary disks are believed to be the birthplaces of planetary moons, such as the Galilean moons that orbit Jupiter. They also may play an important role in our understanding of how planets accumulate their masses. While they are theoretically predicted to surround giant planets at birth, there has been little observational evidence to date for circumplanetary disks outside the solar system.

The candidate planet was discovered serendipitously through the analysis of archival data taken with the Phoenix spectrograph on the Gemini South telescope (Hinkle et al. 2003, Proc. SPIE, 4834, 353). The signature of the candidate planet was confirmed with subsequent spectroscopy obtained with CRIRES, the cryogenic high-resolution infrared echelle spectrograph on the Very Large Telescope.

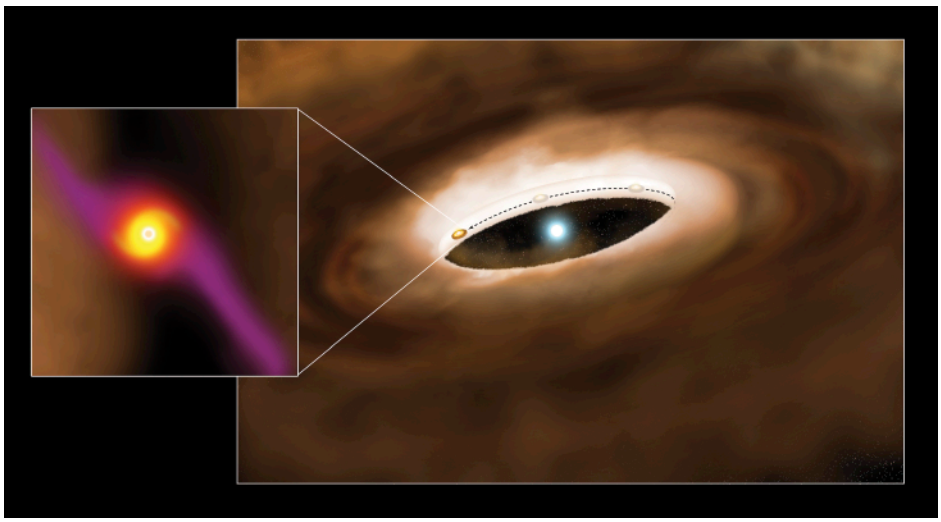

An artist's conception of the young massive star HD100546 and its surrounding disk. A planet forming in the disk has cleared the disk within 13 AU of the star. Gas and dust that flow from the circumstellar disk to the planet surrounds the planet as a circumplanetary disk (inset). Circumplanetary disks are believed to be the birthplaces of planetary moons, such as the Galilean moons that orbit Jupiter. While they are theoretically predicted to surround giant planets at birth, there has been little observational evidence to date for circumplanetary disks outside the solar system. Observations over 10 years trace the orbit of the forming planet from behind the near side of the circumstellar disk in 2003 to the far side of the disk in 2013. These observations provide a new way to study how planets form. (Image credit: Pete Marenfeld/NOAO/AURA/NSF.)

The spectroastrometric technique measures the center of the point spread function (PSF) of a spectrum as a function of wavelength (e.g., Bailey et al. 1998, MNRAS, 301, 161). Because the PSF center can be measured to a much higher accuracy than the diffraction limit of an instrument, spectroastrometry can provide valuable spatial information on small spatial scales when applied to systems with simple velocity fields.

The Brittain et al. study illustrates how spectroastrometry of orbiting gas (e.g., in a circumplanetary disk) may be an alternative way to identify and study forming planets. Other candidate-forming planets identified to date have been identified primarily through direct imaging studies.